agriculture

Article

Dynamic Change in Normalised Vegetation Index (NDVI) from 2015 to 2021 in Dhofar, Southern Oman in Response to the Climate Change

Khalifa M. Al-Kindi [1,*], Rahma Al Nadhairi [2] and Suleiman Al Akhzami [2]

[1] UNESCO Chair of Aflaj Studies, Archaeohydrology, University of Nizwa, Nizwa P.O. Box 33, Oman
[2] Environment Authority, University of Nizwa, Nizwa P.O. Box 33, Oman
* Correspondence: alkindi.k@unizwa.edu.om; Tel.: +968-95218088

Abstract: Climate change poses a major threat to vegetation and land cover worldwide. The loss of vegetation as a result of climate change can alter the functions and structure of the environment and its ecological systems. In the first part of this study, Sentinel-2 data, normalised different vegetation index (NDVI), and multiple regression methods were used to examine the impacts of the climatic factors of humidity, rainfall, and air temperature on vegetation dynamics from 2015 to 2021 in Dhofar, Southern Oman. In the second part of this study, random forest regression was employed to model the relationships between the NDVI and temperature, humidity, rainfall, soil map, geology map, topographic wetness index, curvature, elevation, slope, aspect, distance to buildings, and distance to roads. The multiple regression values revealed significant associations between the spatial distributions of the NDVI and the abovementioned climatic factors. The findings also indicated an increase of 1 °C in air temperature fluctuations between 2018 and 2021 over all five sites, with a strong tendency over Qairoon Hairiti Mountain. The rainfall records clearly indicated an increasing tendency from 2018 to 2020 due to the impact of frequent cyclones. Therefore, the results revealed a significant increase of 0.01 in the vegetation cover trend in 2018, 2019, and 2020 along the Sadah Mountain range and the eastern part of the Jabal Qara Mountains under the areas directly impacted by the cyclone, whereas there was a decrease along the western mountain range consisting of Jabal Qara and Jabal Qamar Mountains due to the impact of warm, dry air. The results revealed that NDVI values were sensitive to heavy rainfall over Jabal Samhan Mountain. The 12 variables that influenced NDVI levels had different levels of importance. Soil types, elevation, slope, rainfall, curvature, humidity, and temperature had the highest importance, while topographic wetness index, distance to urban area, aspect, distance to roads, and geology map had the lowest. The findings provide a significant foundation for Oman's planning and management of regional vegetation, water conservation, and animal husbandry.

Keywords: climate change; Sentinel-2; NDVI; vegetation; Salalah; Sultanate of Oman

check for updates

Citation: Al-Kindi, K.M.; Al Nadhairi, R.; Al Akhzami, S. Dynamic Change in Normalised Vegetation Index (NDVI) from 2015 to 2021 in Dhofar, Southern Oman in Response to the Climate Change. *Agriculture* **2023**, *13*, 592. https://doi.org/10.3390/agriculture13030592

Academic Editor: Francesco Marinello

Received: 5 February 2023
Revised: 25 February 2023
Accepted: 26 February 2023
Published: 28 February 2023

1. Introduction

Through photosynthesis and surface albedo processes, land vegetation cover plays an important role in regulating the carbon cycle in terrestrial ecosystems [1]. Vegetation cover also plays a key role in the economic structure and development of a country or region, particularly in arid and semi-arid areas, where agricultural and livestock production are the main economic activities [2,3]. There are several factors that affect land vegetation, including natural effects (e.g., climate) and human activities [4]. The intensification of human activities and urbanisation have put significant pressure on nature, thereby leading to shortages of natural resources worldwide. Seto et al., 2012 [5] calculated that urbanisation will disrupt 5% of global habitat, biomass, and carbon storage by 2030. A more recent study discovered a high correlation between the vegetation index and the building index, thereby implying that urbanisation has an indirect impact on vegetation in Dhofar's mountains, plains, and coastal areas [6]. The study also found, using a linear methods tool, that urbanisation was responsible for a decline of 18.5% in other plant species found in mountainous areas. Prior studies [7,8] have primarily used linear correlations to illustrate the influence of human activities on vegetation change. Climate change has caused a reduction in plant cover in numerous places around the world, which has had major economic effects and significant losses in biodiversity and the ecosystem [9]. For example, drought afflicted an average of 21 million hectares in China between 1949 and 2000, thereby resulting in a loss of over 60 million tons of grain in 2000, the largest documented loss in 51 years in the country [10]. A recent study in the United States found that global warming had already contributed considerably to the loss of national-level crop insurance to the tune of USD 27.0 billion between 1991 and 2017 [11]. However, a deeper knowledge of vegetation changes and their response to climatic influences is crucial for forecasting future climatic change and vegetation growth and health pattern conditions [12].

Numerous studies have found that global change has had a significant impact on the normalised difference vegetation index (NDVI) worldwide [13–15]. Furthermore, many of the studies conducted at regional levels to investigate the relationship between NDVI and climatic conditions revealed variations in the mechanisms underlying the response of vegetation to climate change due to differences in regions, vegetation characteristics, and study methods [16]. For example, Liu et al. [17] found that vegetation coverage has a high positive correlation with rainfall in the arid western parts of north-eastern Asia, whereas changes in NDVI—which are driven mainly by temperature—are less pronounced. Schultz et al. [18] found that NDVI measurements on a global scale are not strongly associated with rainfall. However, only a few studies have been undertaken on the impact of climate change and its associated vulnerabilities in the Sultanate of Oman [19–21]. For example, a study conducted to compare temperature and rainfall trends between 1980 and 2013 found that Oman was sensitive to climate change [21]. According to the findings, the north of Oman (the non-monsoonal subregion) had the greatest statistically significant warming trends of 0.6 °C per decade^{-1}, whereas the lowest warming trend values were recorded over the monsoonal area of Dhofar and along the southeast coast (0.1 °C per decade^{-1} in Salalah). In terms of total annual rainfall, the results revealed negative trends over Salalah station in southern Oman, with a negative trend of 10.8 mm per decade^{-1}, whereas Saiq station in northern Oman had a negative trend of 74.0 mm per decade^{-1} [21,22]. Furthermore, there was a significant increase in tropical cyclone events in Oman between 2007 and 2021. Among these cyclones were Cyclone Gonu in 2007 [23], cyclone Phet in 2010 [24], Cyclone Mekunu in 2018 [25], and Depression ARB01 in May 2020. Cyclone Mekunu hit the region (Dhofar) with over 500 mm of rain. It caused catastrophic flooding and had an impact on groundwater recharge as well [25].

Despite numerous studies demonstrating global NDVI changes, few studies have been conducted on vegetation cover and NDVI values in response to climate change, particularly in the Dhofar governorate in southern Oman. Galletti et al. [7] reported that between 1988 and 2013, there was a decline in the NDVI in Salalah's coastal plain. However, each of the mechanisms used to scrutinise the relationships between the dependent (NDVI) and independent variables (climate, environmental, and human activities) discussed previously are traditional statistical methods, which occasionally might not fully reflect the complex relationships between NDVI and human, climatic, and situational influences in the study area. We contend that most current research on vegetation cover has concentrated solely on ecology, human activities, or control mechanisms. Because of the lack of an adequate network of monitoring stations, the unsuitability of small areas for cultivation, large areas that are unreachable and uninhabited, and a lack of personnel for effective database management and analysis, and a lack of short-term and specific weather data, analyses on these aspects to study the relationship between the NDVI and climatic factors—such as temperature and humidity—are limited in Oman. There has been very little research linking NDVI spatial and temporal distributions to human, environmental, and meteorological activities that promote its survival and development on a geographical and temporal scale. Understanding the distribution and affinity of the NDVI in terms of these variables, as well as data mapping, can play an important role in its control and management as well as in capacity planning. The data indicate that grazing activities and urbanisation are the principal drivers of these changes.

Thus, this study was carried out to analyse how vegetation in the Dhofar areas responded to climate change from 2016 to 2021 and to examine the spatiotemporal variation vegetation pattern using satellite datasets from Sentinel-2. We structured this study into two parts to fulfil these objectives. The first section of this study looks at individual climate parameters and their relationships with NDVIs. In the second phase of this study, we used more advanced predictive models and regression analytic approaches to investigate the combinations of climate, ecological, and human activity elements that are most conducive to vegetation cover survival. From 2016 to 2021, spatial regression methods were employed to investigate the effects of climate parameters such as air temperature, humidity, and rainfall on vegetation dynamics. To model and predict the interactions between the NDVI and temperature, humidity, rainfall, soil type, geology types, topographic wetness index (TWI), curvature, elevation, slope, aspect, distance to buildings, and distance to roads, Random Forest Regression (RFR) was utilised.

2. Materials and Methods

2.1. Study Area

The study area was located in southern Oman and extended from 16° N–18.5° N to 52.5° E–55.5° E. Salalah is the capital city and is located in the southern region of Oman. It is bound on the southeast by the Arabian Sea, on the south by the Republic of Yemen, and on the northwest by the Empty Quarter Desert (Figure 1). The area is distinguished by its complex terrain, which divides it into two physiographic zones: (1) the mountain ranges of Jabal Samhan, Jabal Qara, and Jabal Qamar, and (2) the Salalah plain. The elevation rises abruptly from the flat coastal plain to approximately 2100 m in the mountain ranges (Figure 1). The climate is generally arid, with cooler summers here than in the northern or inland parts of Oman. Moreover, the region is affected by south-westerly winds in the summer, which cause an upwelling of cold seawater off the coast, thereby causing the air temperature to reduce to 18 °C and the average rainfall to increase to 100 mm [26,27]. In winter, winds from the northeast influence the temperature in the area, with the average temperature varying between 18.8 °C and 28.7 °C.

Salalah Plain is regarded as a pillar of economic growth in the Sultanate, and its crops (coconut, papaya and bananas) contribute to the productivity of the agricultural sector [28]. The city is rich in natural plants that cover the mountains tops and spread across the valleys and plains; many of these plants were well-known in the past for their various uses and benefits, whether these were food, medicine, or a source for numerous industries and businesses. The frankincense tree is one of the most important plants in the Salalah plain, where it has historical significance and serves as a link to ancient civilisations. In addition, 76 species of rare plants that are not found anywhere else in the world have been recorded to be found here. The primary biomes formed due to the intermixing of the three most prevalent natural land coverings are forests, shrublands, and grasslands. The forests are typically found in high altitudes in the mountains and wadis areas (river valleys).

Drought and upcoming water shortages are becoming more commonplace due to climate change. The effectiveness of climate change adaptation will ultimately depend on the commitment made through programmes and regulations in the context of sustainable development. Consequently, it is essential to examine the present conditions to plan current and future investment models [29].

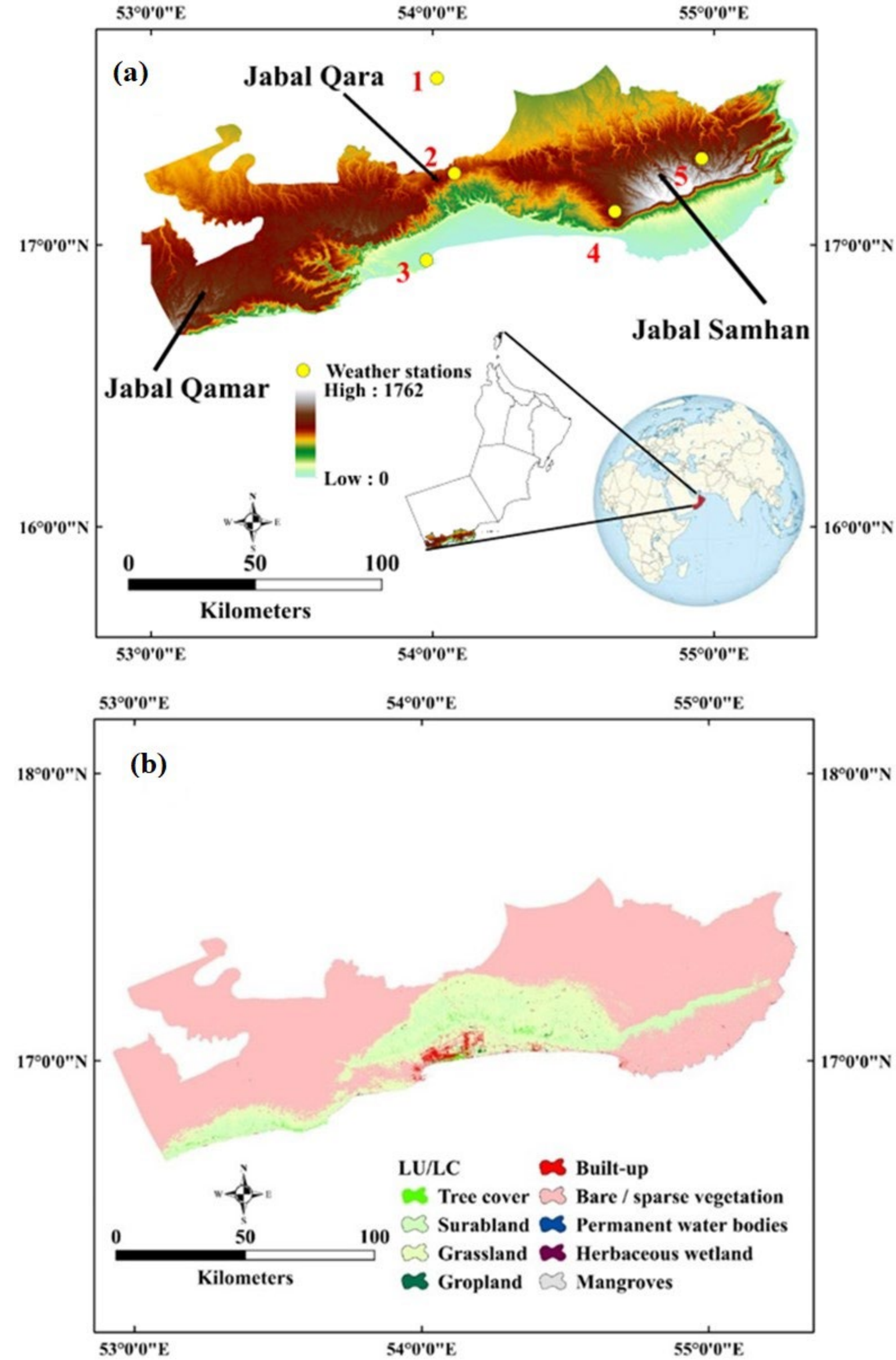

Figure 1. The study area: (**a**) the Dhofar elevation map with weather station locations and the Dhofar portion of the Salalah plain and mountain ranges (Jabal Qara, Jabal Qamar, and Jabal Samhan). (**b**) Data from Sentinel-2 indicate the land use and land cover zones in the study area.

2.2. Data Sources and Analysis

2.2.1. In Situ Meteorological Data

There are a few weather monitoring stations scattered throughout the Governorate of Dhofar (Table 1). Five stations (Mirbat, Qairoon Hairiti, Sadah, Salalah Port, and Thumrait) were selected to examine trends in air temperature, relative humidity, and rainfall from 2016 to 2021. Data from two of the five stations, one coastal (Salalah Port) and the other mountainous (Qairoon Hairiti), were analysed for correlations between the observation data and the ERA5 model (Table 2). All weather data were obtained from the Civil Aviation Authority (https://www.caa.gov.om (accessd on 25 October 2012). Furthermore, the inverse distance weight (IDW) in ArcGIS Pro 2.8 was used to estimate the spatial pattern of average rainfall, humidity, and temperature in the study area. The IDW method is a predetermined interpolation method that creates a smooth surface by fitting a mathematical function to input data [30]. By synthesising the NDVI surface and the surfaces corresponding to the various climate variables, data were extracted to investigate the correlations among the layers.

Table 1. Longitude and altitude for different observing stations over Dhofar.

No.	Station	Longitude	Latitude	Elevation (m)
1	Thumrait	54.024	17.681	448
2	Qairoon Hairiti	54.084	17.256	881
3	Salalah Port	54.008	16.934	24
4	Mirbat	54.773	16.966	16
5	Sadah	55.056	17.100	88

Table 2. Annual 2-metre air temperature and total rainfall over Salalah Port and Qairoon Hairiti station.

Year	Air Temperature (°C)		Total Precipitation (mm)	
	Salalah Port	Qairoon Hairiti	Salalah Port	Qairoon Hairiti
2000	25.7	22.0	0	0.8
2001	25.4	21.4	0.2	0
2002	25.5	20.7	181.4	348.8
2003	26.0	20.8	70.4	76.4
2004	25.6	20.8	184.4	248.2
2005	25.7	20.5	112.6	175.4
2006	25.9	20.7	112.2	163.8
2007	26.2	21.4	132.4	154
2008	25.2	20.6	102.8	90.6
2009	26.1	17.2	59	0.4
2010	26.2	21.6	78.8	10.2
2011	25.8	21.0	162.2	385.4
2012	25.9	21.4	44	101.8
2013	26.0	21.2	79.6	203.4
2014	26.2	21.2	72	96.8
2015	26.5	21.5	47	89.4
2016	26.2	21.4	90	78.4
2017	26.5	21.4	54.4	2.2
2018	25.9	21.2	1366	510.8
2019	26.9	21.5	59.4	145.6
2020	26.5	22.1	135	500.0
2021	26.3	22.7	67	70

2.2.2. Trends Analysis of Climatic Factors

One of the commonly used statistical methods to examine trends in climatic factors is linear regression. A simple linear regression model involves the following equation:

$$y = a + bx \quad (1)$$

where "y" refers to the dependent variable, which represents the climatic factor being evaluated, and "x" represents the independent variable, usually representing time, such as a year. "a" signifies the intercept, or the value of "y" when "x" is zero, whereas "b" denotes the slope, which represents the rate of change in "y" concerning "x". The equation was used to estimate the connection between the climatic factor and time and determine the trend in the climatic factor over time [31,32]. A positive slope means an upward trend, while a negative slope indicates a downward trend in the climatic factor over time. The magnitude of the slope signifies the rate of change in the climatic factor over time. The equation can also be utilised to predict future values of the climatic factor by examining past trends. Overall, the trends analysis of climate factors shows that climate change is happening at an unprecedented pace, requiring urgent action to mitigate its impacts.

2.2.3. ERAS Model Data

The ERA5 model is the fifth and most recent generation of European reanalysis generated by the European Centre for Medium-range Weather Forecasts (ECMWF), and is a crucial component of the Copernicus Climate Change Services [33]. It computes atmospheric variables at 139 pressure levels and has a horizontal resolution of approximately 30 km. It began operating on 1 January 1979 and has been continuously extended forward in almost real time. ERA5 reanalysis combines in situ observation, satellite data and model forecasts in data assimilation techniques to provide a reliable description of the climate. The ERA5 model produces a 2 m air temperature. Furthermore, monthly ERA5 products of air temperature and total rainfall were obtained from the Copernicus climatological data store (https://cds.climate.copernicus.eu (accessed on 30 December 2020)). The ERA5 model dataset with a 0.250 resolution is rather useful for capturing the different patterns of rainfall, air temperature, and drought predictions on an annual and seasonal basis. The model also enables decision makers to collect more precise information on the impacts of climate change on the area and land status [34]. However, to investigate the impacts of climate change on various plant species, higher-resolution numerical models are required, and this research study will be further developed in this regard in the future. The model had a resolution of $0.25 \times 0.25°$ and covered the period from 1 January 2000 to 31 December 2020. It is based on models and satellite record observations and is sufficiently precise for meteorological applications, particularly when surface measurements are unavailable [35–37]. In this study, the ERAS model was used to analyse temperature, humidity, and rainfall patterns over a vast scale of the study area.

2.2.4. NDVI Trends Based on Sentinel-2 Data

Sentinel-2 satellite cloud-free images were acquired six times between 2016 and 2021 (https://earthexplorer.usgs.gov (accessed on 30 October 2021)). Sentinal-2 is equipped with electrical, optical spatial, and spectral sensors with a spatial resolution of 10–60 m in the visible, near-infrared, and short-wave infrared spectral zones (13 spectral bands), thereby permitting detection of differences in vegetation structure conditions—including temporal changes—while minimising the impact on atmospheric photography quality [38,39]. The images were georeferenced to the World Geodetic System 1984, projected into the UTM Zone, and processed using ArcGIS Pro 3.0. The NDVI measures reflectance in near-infrared [40,41]. NDVI values can be calculated in the following manner:

$$\mathrm{NDVI} = (\mathrm{P(NIR)} - \mathrm{P(R)})/(\mathrm{P(NIR)} + \mathrm{P(R)}) \quad (2)$$

where Red and NIR are spectral reflectance in the red and near-infrared wave satellite bands, respectively [42]. The data processing system went into operational status to enable updates on a global scale with an implemented validation data collection system. In this study, NDVI data from October with a resolution of 10 m were selected for the period from 2016 to 2021 (http://land.copernicus.eu/global (accessed on 30 October 2021)). In certain regions, the month of October is commonly used for NDVI analysis due to the reduced cloud cover and atmospheric moisture, which can result in clearer and more dependable data. This makes it easier to detect changes and patterns in vegetation growth. Nonetheless, the selection of the specific time period for NDVI analysis should take into consideration other environmental factors that may influence vegetation growth, such as temperature, soil moisture, and the timing of the rainy season. While selecting October for NDVI analysis based on low cloud cover is a valid option, it is crucial to consider other pertinent factors and to employ appropriate methods for analysing the data [38,43,44]. NDVI data were then used to analyse changes in vegetation cover and model the trend relationships with climatic factors (rainfall, humidity, and temperature) in the study area.

2.2.5. NDVI Trends Based on Proba-V Satellite Data

One of the widely used methods for ecological and environmental research is analysing the trends in Normalised Difference Vegetation Index (NDVI) with the help of satellite data. Proba-V is a dedicated satellite mission that focuses on monitoring the growth of vegetation, which makes it an excellent resource for studying changes in plant life over extended periods of time [45,46].

To analyse trends in NDVI using Proba-V satellite data, we first obtained and preprocessed the satellite imagery, calculated NDVI values using appropriate software and the NIR and RED bands of the imagery, and used linear trend (slope) test to analyse the temporal trends.

2.2.6. NDVI Condition Factors

The distribution and health of vegetation can be influenced by a range of environmental variables, such as elevation, soil types, slope, aspect, topographic wetness index, geology types, curvature, temperature, rainfall, humidity, and distance to urban areas and highways. For example, elevation can affect temperature and precipitation patterns, which can impact vegetation growth and survival, while soil types can affect nutrient availability and water retention, which are crucial for photosynthesis and growth. Slope and aspect can influence the amount and quality of sunlight reaching the vegetation, which can impact photosynthesis rates and overall health, and TWI can influence the water content of soil, which is important for plant growth and survival. Geology types can impact the types and availability of nutrients in the soil, and curvature can affect the amount of sunlight and water that reaches the vegetation [47–50]. In general, understanding the interactions between these environmental variables and vegetation is important for predicting and mitigating the effects of environmental change on vegetation. By analysing the relationships between NDVI and these environmental variables, we can gain insights into how vegetation responds to environmental changes and identify strategies for promoting healthy and resilient vegetation in the face of future environmental changes.

To analyse the environmental variables affecting vegetation and their spatial distribution, the study employed various methods. Initially, the Digital Elevation Model (DEM) was utilised using ArcGIS Pro 3.3 to derive key factors such as slope, aspect, curvature, and topographic wetness index. The IDW method was also employed to predict the spatial distribution of rainfall, temperature, and humidity. Furthermore, the Euclidean distance method was used to determine the distance from urban areas and roads to better understand their impact on vegetation. The DEM, which has a 5 m two-dimensional resolution, was acquired from the National Survey Authority in Oman using light detection and ranging (LiDAR) data (http://nasom.org.om (accessed on 22 November 2021)).

Geological maps and soil types were obtained from The Ministry of Agriculture, Fisheries Wealth & Water Resources in Oman (https://www.maf.gov.om (accessed on 30 October 2021)), and weather data were sourced from the Civil Aviation Authority (https://www.caa.gov.om (accessed on 27 February 2022)). All indicator factors were georeferenced to the World Geodetic System 1984, projected into the UTM Zone, and processed using ArcGIS Pro 3.0.

2.3. Spatial Relationships Analysis

2.3.1. Spatial Ordinary Least Square

To explain the overall spatial relationships (spatial stationarity) between the explanatory climate variables and the dependent NDVI, the traditional ordinary least square (OLS) regression was employed. OLS was used to investigate the spatial correlations between NDVI and climate variables (temperature, humidity, and rainfall) in order to comprehend the climatic factors underlying the observed spatial patterns and anticipate NDVI-related spatial outcomes based on historical weather stations from 2016 to 2021 [51].

2.3.2. Multivariate Correlation Coefficient and Forest-Based Classification and Regression

The multivariate correlation coefficient method is a statistical technique that can be used to explore the relationships between multiple continuous environmental variables. It assesses the strength and direction of linear associations among variables, providing insights into how changes in one variable might affect others. This method involves creating a correlation matrix that shows the pairwise correlations between all variables, which can be visualised as a heatmap. The multivariate correlation coefficient method is particularly useful in environmental studies with many variables, such as ecology, meteorology, and climatology [52,53].

The study employed multivariate correlation coefficient method to investigate relationships between multiple continuous environmental variables, including soil type, elevation, slope, aspect, humidity, temperature, rainfall, geology curvature, distance to roads, distance to settlements, and topographic wetness index. The authors also utilised a forest-based classification and regression (FBCR) method to analyse the geographic relationships between the dependent variable (NDVI) and the independent environmental variables. FBCR generates a model from known values in a training data set that can then be used to estimate unknown parameters in a prediction database that has the same explanatory elements. This method adapts Leo Breiman's random forest technique, a supervised machine learning method, to develop models and forecast outcomes [54–56]. It produces a large number of decision trees, referred to as an ensemble or a forest, that are utilised to make predictions. Each tree generates its own forecast, and all the forecasts then put through a voting method to decide the final projections. The final forecast is based on the entire forest as opposed to any one tree. This reduces the possibility of over-fitting the model to the training data set, which occurs when a random subset of the training data and a random subset of explanatory variables are used in each forest tree [57,58].

3. Results

3.1. Trend Analysis of Climatic Factors

Figure 2a depicts the change in the mean annual air temperature from in situ ground observation stations in the Dhofar Governorate between 2015 and 2021. In comparison with the mountainous region stations, air temperature records revealed high values in stations in Thumrait, Mirabat, and Salalah Port in the range of 26–28 °C.

Air temperature recorded over mountainous regions indicated low values in the range of 23–24 °C (Figure 2a). Due to global warming, air temperature values increased significantly at all in situ observation stations (~1 °C) between 2018 and 2020, followed by a decrease in 2021 at Thumrait, Mirabat, and Salalah Port stations.

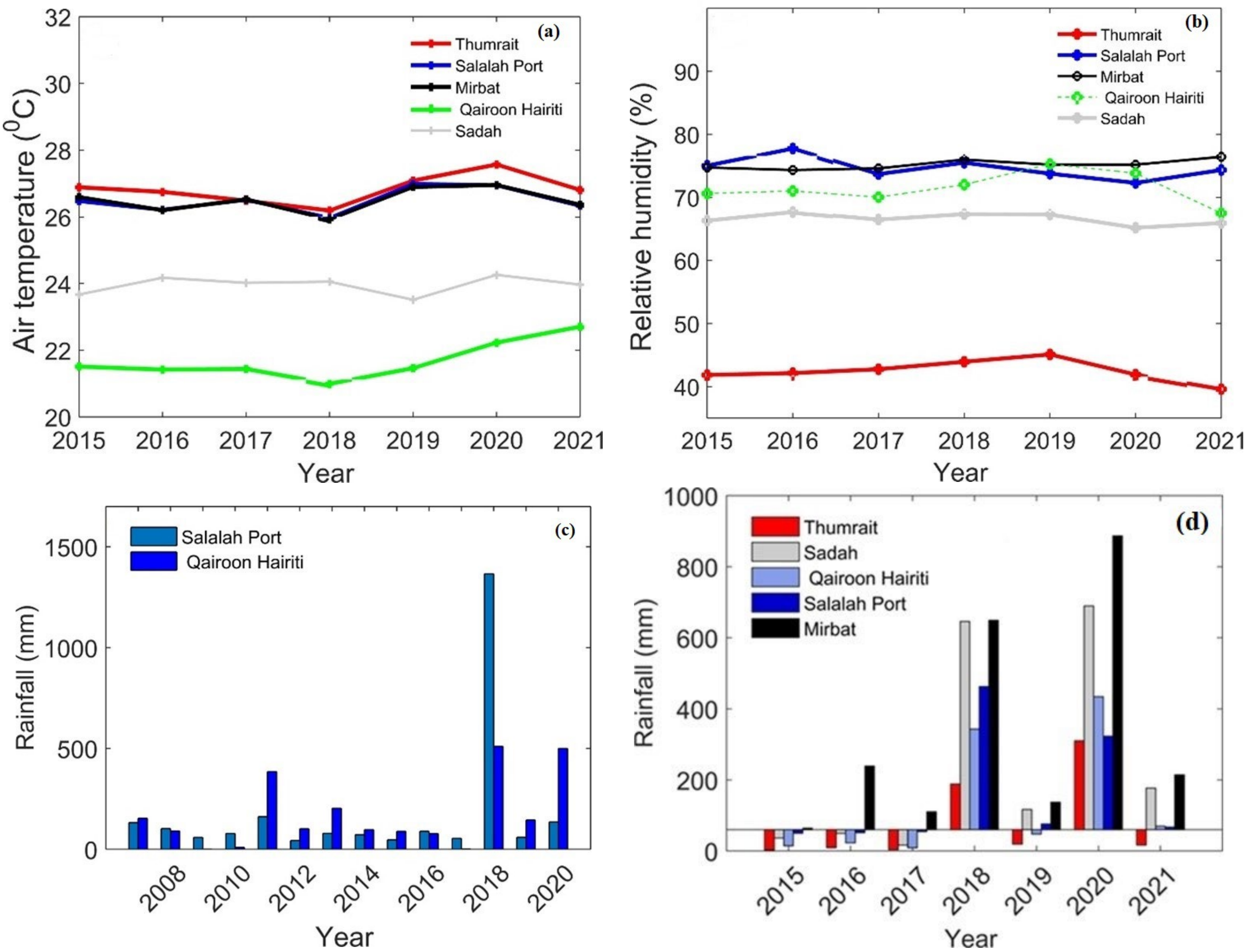

Figure 2. (**a**) Annual variations in air temperature from in situ observation, (**b**) variations in annual relative humidity from in situ observation, (**c**) annual accumulation of rainfall (mm) from in situ observation (Qairoon Hairiti and Salalah Port), and (**d**) total accumulation of rainfall from the ERA5 model.

These observation records confirmed the World Meteorological Organisation's provisional statement that 2016, 2019, and 2020 were the top three warmest years. The trend results of air temperature in the Dhofar Governorate are summarised in Table 3. The observed air temperature trends for the period 2015–2021 reveal large differences between stations (Table 3). We observed that the annual average air temperature trends rose at a rate of 0.01 $^{\circ}$C/year^{-1}, 0.05 $^{\circ}$C/year^{-1}, 0.04 $^{\circ}$C/year^{-1} in Sadah, along coastal area stations in Salalah Port and Mirbat, respectively. The Qairoon Hairiti and Thumrait stations showed the highest trends at the rates of 0.187 $^{\circ}$C/year^{-1} and 0.072 $^{\circ}$C/year^{-1}, respectively.

Table 3. Annual trend of air temperature from observation stations during 2016–2021.

Station	Trend (θ Slope)
Thumrait	0.07
Qairoon Hairiti	0.19
Salalah Port	0.05
Mirbat	0.04
Sadah	0.01

Furthermore, the relative humidity values (Figure 2b) increased in Salalah Port from 72% to 75% and 70% to 75% in Mirabat from 2016 to 2019. In Qairoon Hairiti station, these values increased from 70% to 75% between 2018 and 2020, then decreased to 70% in 2021. Thumrait is an inland city approximately 80 km north of Salalah, with an average low humidity ~40%, a value that has dropped dramatically since 2019. Cyclone Mekunu in May 2018 and Depression ARB01 in 2020 caused significant increases in rainfall over 1000 mm in Salalah Port and 500 m in Qairoon Hairiti [25]. The increasing rate of rainfall from the observations (Figure 2c) coincided with the results from the ERA5 model in Figure 2d. The total rainfall trends from the ERA5 model are summarised in Table 4. Annual rainfall accumulation has a trend of 100 mm/year^{-1} in Mirbat and Sadah stations (Table 4), whereas Sadah station had a trend of 72 mm/year^{-1}. The lowest trend of annual rainfall accumulation was observed in Thumrait inland station, with a value rate of 50 mm/year^{-1} and at Salalah Port with a rate of 53 mm/year^{-1}.

Table 4. Annual trend of rainfall accumulation from 2015–2020 obtained from the ERA5 model.

Station	Trend (θ Slope)
Thumrait	50
Qairoon Hairiti	72
Salalah Port	53
Mirbat	124
Sadah	117

3.2. Analysis of ERA5 Model of Air Temperature and Total Rainfall

The findings of the ERA5 model for air temperature and total rainfall are presented in Figure 3. The model results revealed high mean annual air temperature values, exceeding 27.5 °C in inland areas (Figure 3a), with a decline in temperature across the mountain range, with a mean value of 23 °C.

Figure 3b depicts the differences in the annual mean air temperature for the period between 2019 and 2015; it reveals contrasts in air mass characteristics with a high rate of air temperature change (0.4 °C) in inland dry areas that extend into Salalah Port and Qairoon Hairiti. This is primarily due to dry, warm inland air. Furthermore, the rate of mean annual air temperature change was slow (0.2 °C) along the coast of Jabal Qamar, the eastern coast of Salalah Port and Samhan Mountain. This is due to the cold upwelling water during the summer monsoon, which slows the rate at which the air temperature rises. Total rainfall accumulation results revealed high annual mean rainfall values along the eastern coastal areas of Salalah Port during the 2015–2017 monsoon season in the range of 400–600 mm (Figure 3c). Cyclone Mekunu in 2018 and Depression ARB01 in 2020 both hit the eastern part of the Dhofar Governorate, dumping over 1000 mm of rain in the eastern part of Salalah Port and ~800 mm in the western part of the port (see Figure 3d).

3.3. Spatial and Temporal Trends of NDVI and Its Degree of Change

Figure 4 depicts the October 2015 NDVI (Normalised Difference Vegetation Index) values across the study area, with a small box highlighting the contrast between forested areas (dark green) and grasslands (light green). Meanwhile, Figure 5 illustrates the spatiotemporal distribution of NDVI values over the period of study, which spans from 2016 to 2021. The spatial destinations of the NDVI values were examined using Sentinel-2 remote sensing data. We found that the peak NDVI values ≥ 0.5 were located in the mountain ranges of Jabal Qara and Jebel Qamar, and minimum values < 0.1 occurred along the flat coastal plain. We also found a low level of NDVI values along the highest peaks of Jabal Samhan Mountain. Forests are typically found at high altitudes in the mountain ranges of Jebel Qamar and Jabal Qara. Figure 6a–f depict the spatial–temporal distribution differences in the NDVI mean values in October between 2015 and the years between 2016 and 2021. Overall, the difference in NDVI mean values between 2016–2015 and 2016–2017 was high in the Jabal Qamar and Qara Mountains, ranging from 0.5 to 0.8 (Figure 6a,b).

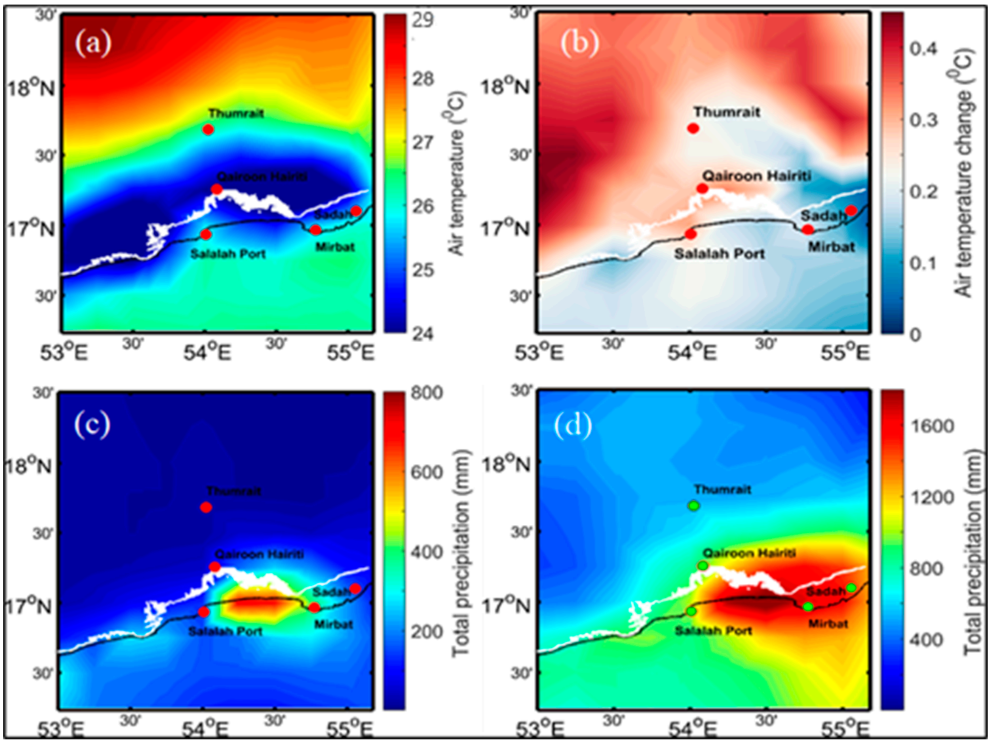

Figure 3. ERA5 model results: (**a**) spatial distribution of annual air temperature (°C) for the period of 2015–2017, (**b**) change in air temperature between 2015 and 2019, (**c**) total annual rainfall (mm) accumulation for the period 2015–2017, (**d**) total annual rainfall (mm) accumulation for the period 2018–2020. The white-coloured line depicts the mountain peaks' border.

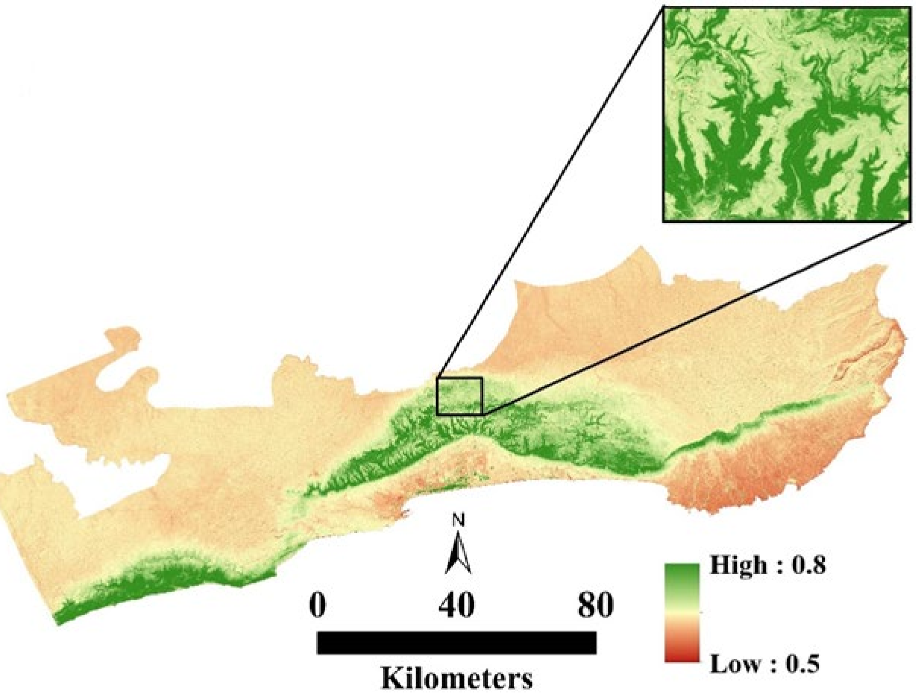

Figure 4. The spatial distribution of NDVI values for October 2015; the small box indicates the contrast between forests (dark green) and grasslands (light green).

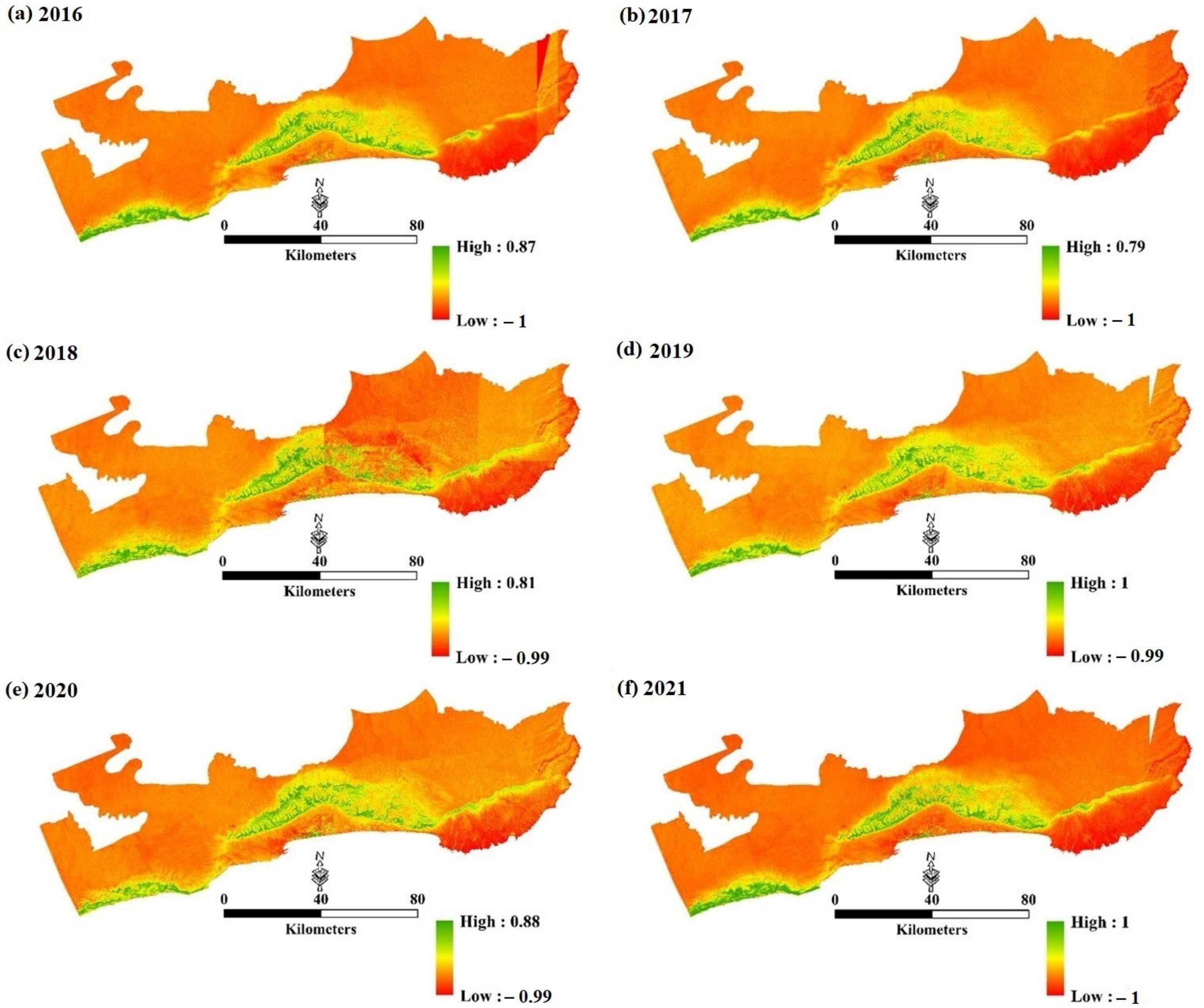

Figure 5. Displays how NDVI values varied over time and space across the study area during the period from 2016 to 2021 (**a**–**f**).

Cyclone Mekunu caused an increase of 0.4 in the rate of change in NDVI values along the Jabal Samhan Mountain range between 2018 and 2015, whereas this rate decreased in the Jabal Qamar Mountain range (Figure 6c). However, the difference in NDVI values from 2019 to 2015 indicated slight improvements on the western side of the Dhofar Governorate in the Jabal Qamar Mountain range and decreased in the eastern part along Jabal Samhan Mountain (Figure 6d).

There was a sharp decrease in the difference in NDVI values for the period 2020–2015 over Jabal Qamar Mountain—approximately −0.8 in the Jabal Qamar Mountain and an increased rate of ~0.5 over Jabal Samhan Mountain (Figure 6e). However, in 2021, there was an increase in the NDVI values over Jabal Samhan Mountain, whereas there was an increased in these values over Jabal Qamar Mountain (Figure 6f).

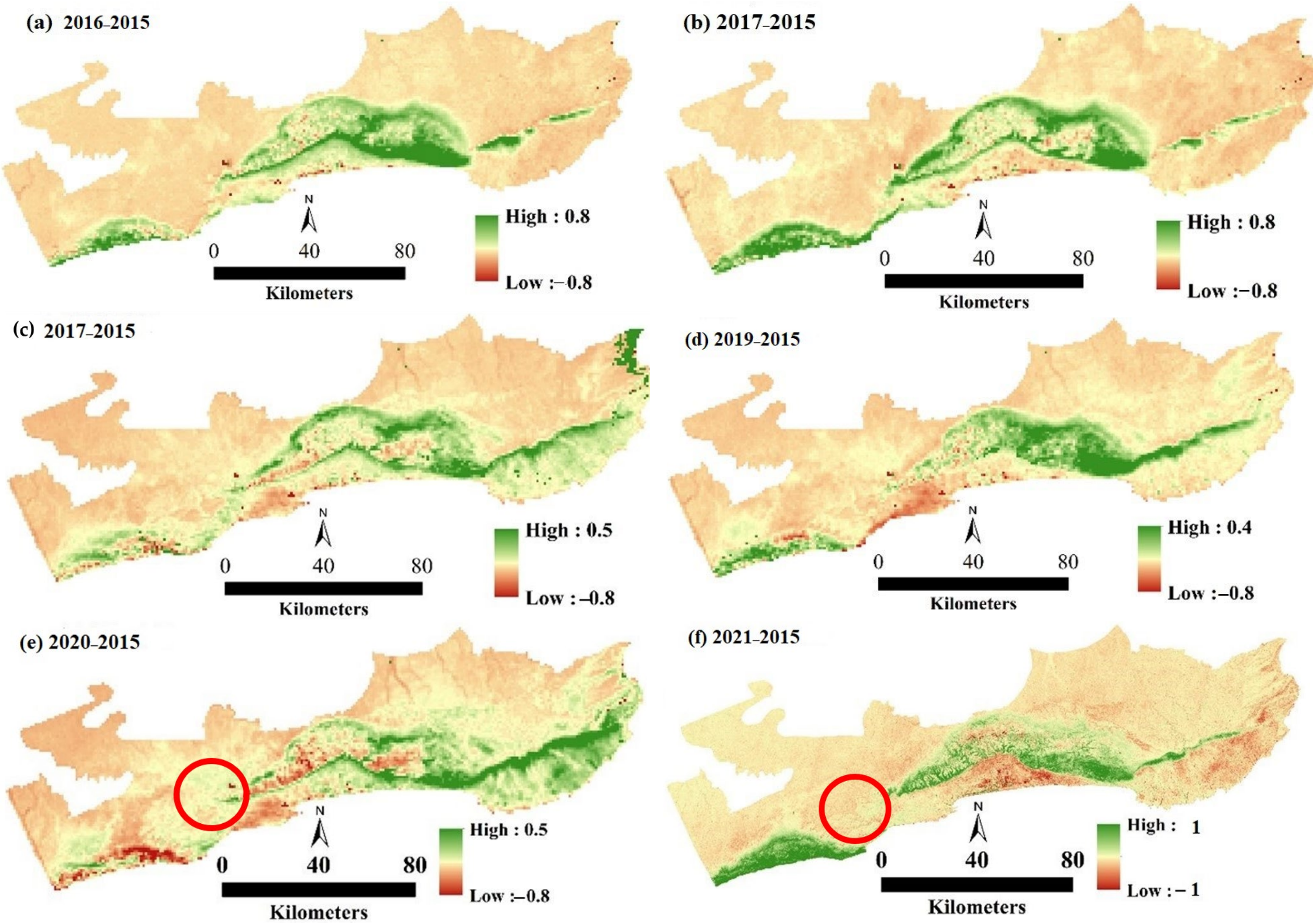

Figure 6. The difference in mean NDVI values in the month of October over Dhofar: (**a**) 2016–2015, (**b**) 2017–2015, (**c**) 2018–2015, (**d**) 2019–2015, (**e**) 2020–1015, and (**f**) 2021–2020.

3.4. NDVI Trend Analysis Based on Proba-V Satellite Data

Using the continuous long-record data from the Proba-V satellite, the NDVI trend from 2016 to 2020 was calculated, as depicted in Figure 7. The variation trend of NDVI (θ slope) in the study area was divided into five grades [59], as presented in Table 5.

Table 5. Annual mean trend of NDVI for the month of October during the period 2015–2020.

Dynamic Trend	θ Slope
Significant increase	$0.0043 \leq \theta \leq 0.0540$
Slights increase	$0.0009 \leq \theta \leq 0.0042$
No obvious change	$-0.0007 \leq \theta \leq 0.0008$
Slight decrease	$-0.004 \leq \theta \leq -0.0008$
Significant decrease	$-0.1267 \leq \theta \leq -0.0041$

Overall, there was mostly a significant increase in NDVI over Jabal Samhan Mountain and over the eastern part of Jabal Qara Mountain, with a trend value ~0.01. The NDVI of vegetation revealed a slight decrease in the western part of the Jabal Qara and Jabal Qamar Mountains, with a value range ~0.004.

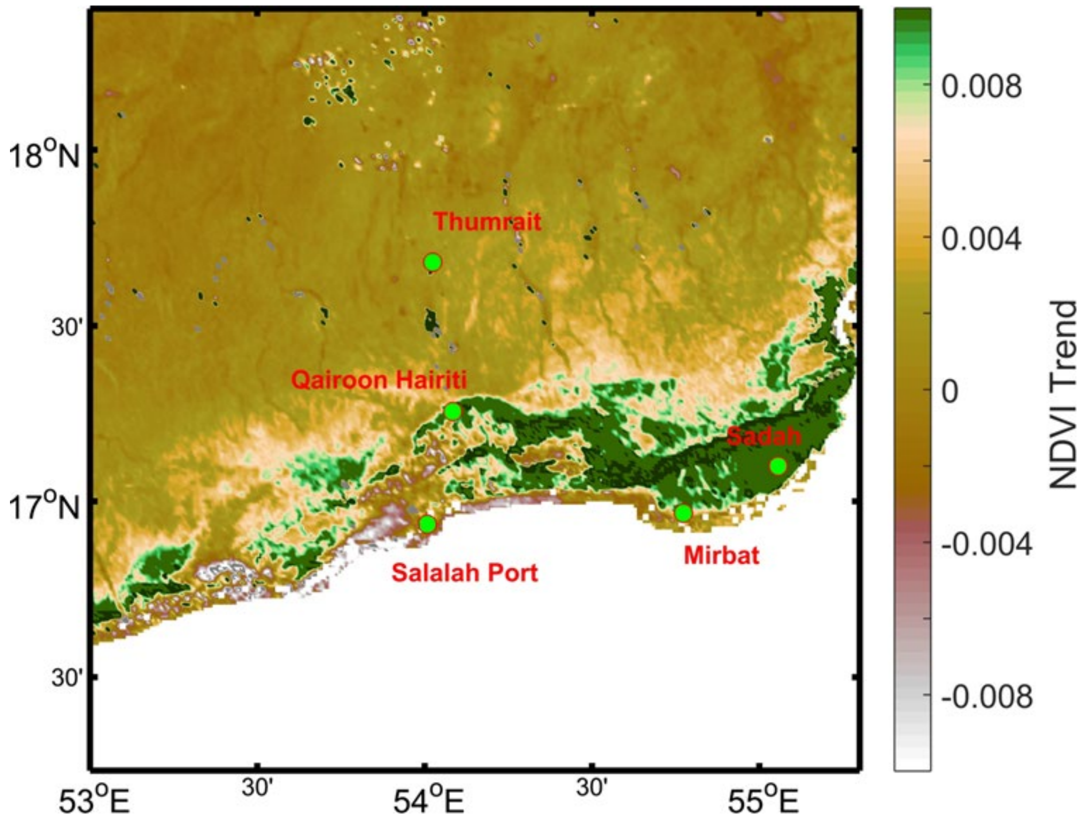

Figure 7. NDVI trends in the study area during the period 2015–2020. Data obtained from the Proba-V satellite.

3.5. Findings from the Regression and Prediction Analyses

3.5.1. Spatial–Temporal Relationships between NDVI and Climate Variables

Figure 8 depicts the relationships between NDVI and climatic factors. Overall, for the six-year model (2016–2021), multiple linear regression using the OLS model revealed that the NDVI values were significantly positively correlated with average annual temperature, rainfall, and humidity factors. Moreover, there was a general trend of strong linear relationships between NDVI levels and climatic factors, with varying coefficients of determination R^2 (Figure 8). The multiple regression model confidently predicts 97% for the period 2016–2019, 99% for 2020, and 97% in 2021.

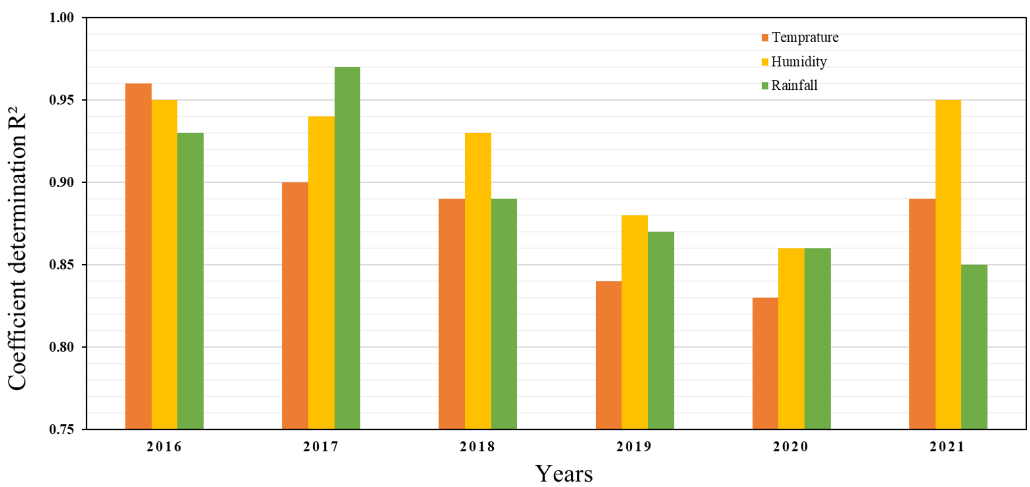

Figure 8. Coefficient is calculated between NDVIs and climate parameters for the years 2016–2021.

3.5.2. Selected NDVI Variables, Forest-Based Classification (FBCR) and Regression Findings

This study examined 12 significant NDVI variables: elevation (Figure 9a), soil types (Figure 9b), slope (Figure 9c), aspect (Figure 9d), topographic wetness index (Figure 9e), geology types (Figure 9f), curvature (Figure 9g), temperature (Figure 9h), rainfall (Figure 9i), humidity (Figure 9j), distance to urban area (Figure 9k), and distance to highways (Figure 9l).

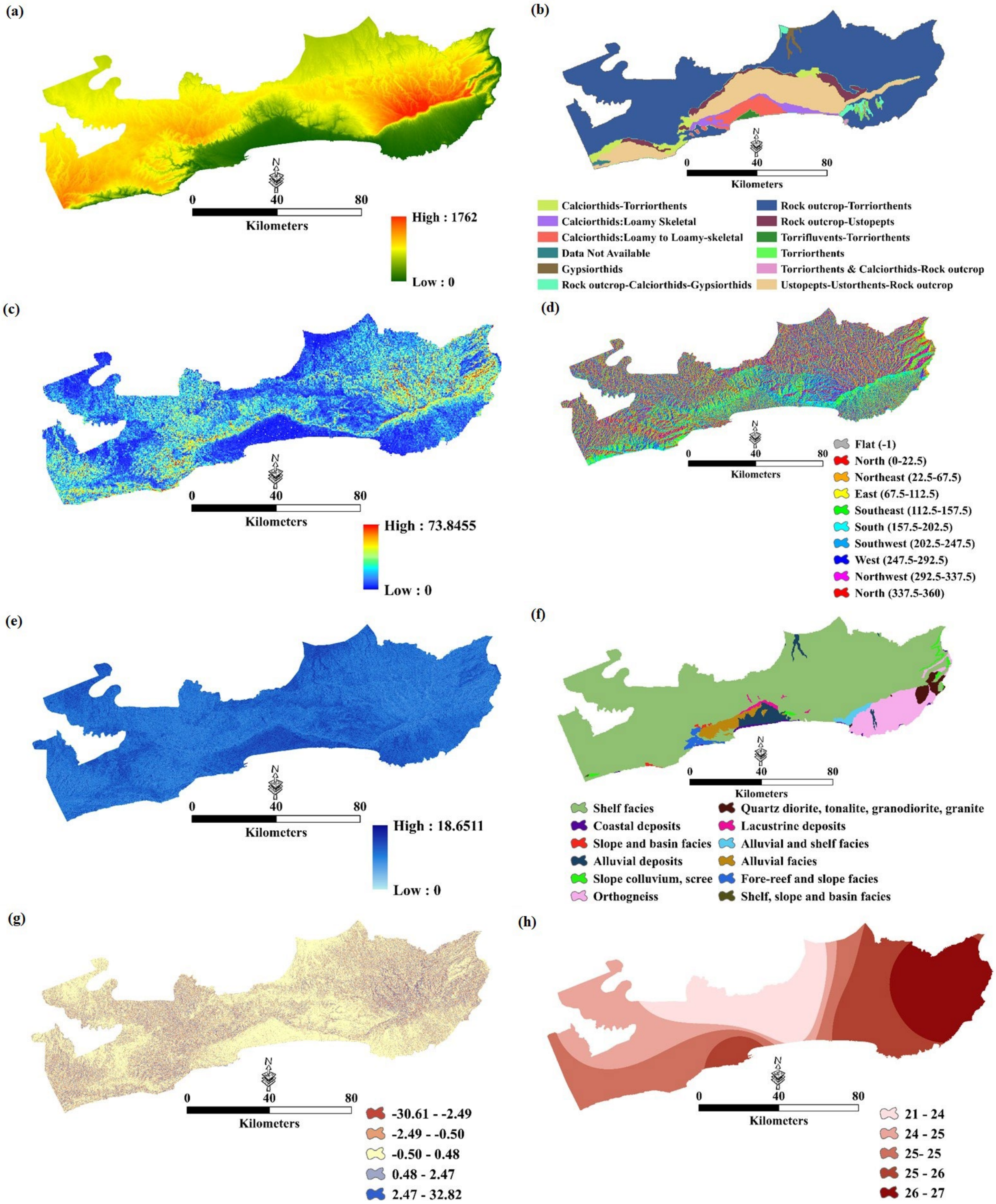

Figure 9. *Cont.*

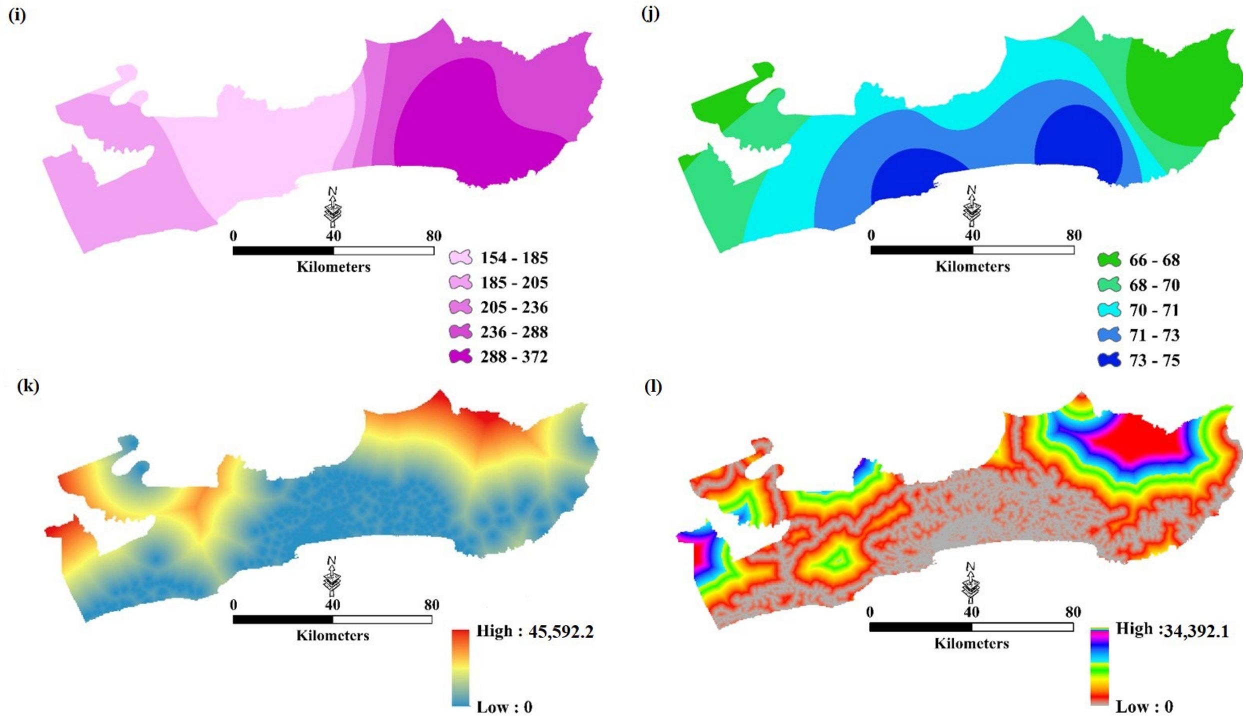

Figure 9. Spatial distribution of the NDVI condition factors: (**a**) elevation, (**b**) soil map, (**c**) slope, (**d**) aspect, (**e**) topographic wetness index, (**f**) golgoy map, (**g**) culvature, (**h**) temperature, (**i**) rainfall, (**j**) humidity, (**k**) distance to urban area, and (**l**) distance to roads.

Our research uncovered strong spatial correlations among several environmental variables, including slope, elevation, rainfall, curvature, aspect, humidity, temperature, distance to roads, distance to urban areas, soil types, geology types, and topographic wetness index. These correlations suggest that these variables play important roles in determining vegetation cover and health within the study area. Our predicted coefficients for these environmental parameters are presented in Figure 10.

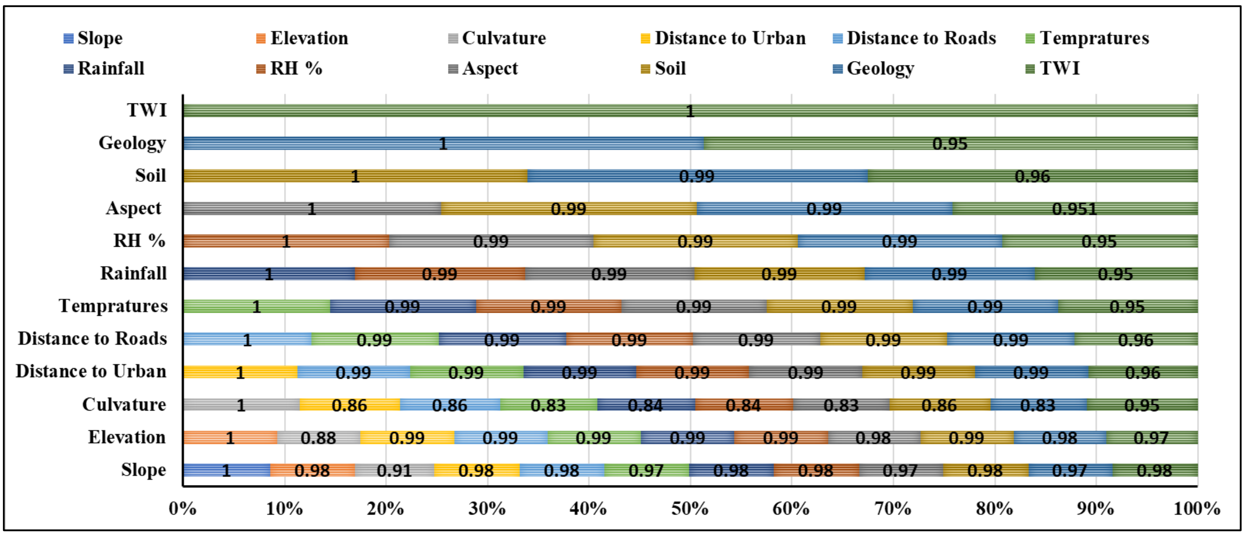

Figure 10. Predicted coefficients for various environmental parameters, including slope, elevation, rainfall, curvature, aspect, humidity, temperature, distance to roads, distance to urban areas, soil types, geology types, and topographic wetness index, which are strongly correlated with vegetation cover and health within the study area.

The findings of the FBCR model's training and validation for relationships between the dependent variable (NDVI) and the independent variables (temperature, humidity, rainfall, soil types, geology types, topography wetness index, curvature, elevation, slope, aspect, distance to buildings, and distance to roads) had high accuracy according to Breiman's random forest algorithm criteria (0.92). The validation result revealed that the forest-based classification was highly effective in modelling the relationships between NDVI and climatological, ecological, and human activities variables. The results of the importance of the relationships between the dependent variable and independent variables based on the forest-based classification and regression method are presented in Table 6. Furthermore, the 12 variables that influenced NDVI levels had different levels of importance. Soil types, elevation, slope, rainfall, curvature, humidity, and temperature had the highest importance, while topographic wetness index, distance to urban area, aspect, distance to roads and geology had the lowest (Table 6). Figure 11 depicts the correlations between NDVI levels derived using forest-based categorisation and the regression model. Each independent variable's link with NDVI levels was given as a probability range from 0 to 1. Based on the natural break approach in ArcGIS Pro 3.0, this chance was graded as very low, low, moderate, high, and very high. The most suitable areas for vegetation based on selected independent variables were in the central and southern portions of Salalah as well as the southern portions of Rakyhut and Dalkat (Figure 11).

Table 6. Importance of variables in the relationships between NDVIs and combinations of climatological, environmental, and human activities factors.

Variable	Importance	%
Soil map	2.0	18
Elevation	1.70	15
Slope	1.68	15
Rainfall	0.98	9
Curvature	0.83	7
Humidity	0.72	6
Temperatures	0.70	6
Topographic wetness index	0.63	6
Distance to urban area	0.57	5
Aspect	0.55	5
Distance to roads	0.51	5
Geology map	0.26	3

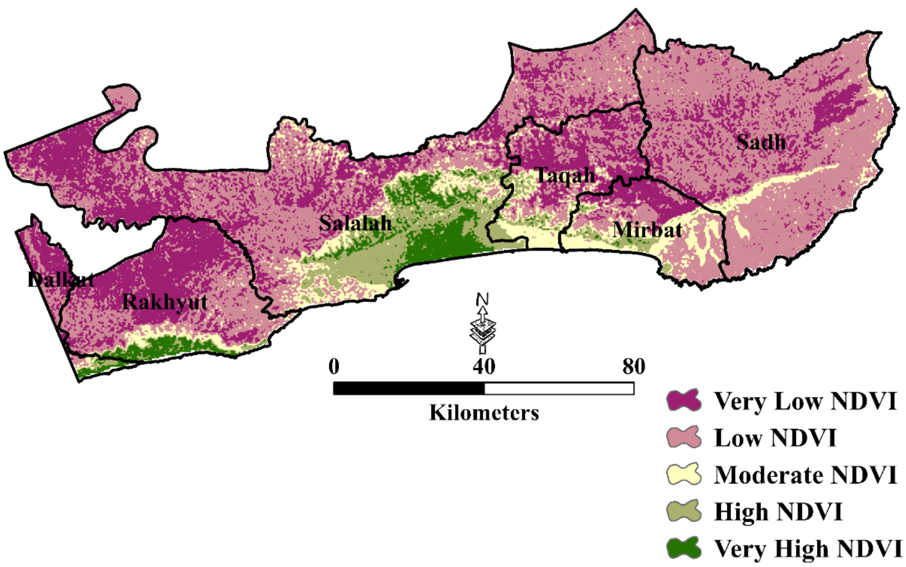

Figure 11. The best areas for vegetation based on the FBCR model.

4. Discussion

The vegetation ecosystems in the Dhofar Governorate exhibit a series of spatiotemporal variations as a result of global climate change, which has a direct impact on the ecological environment. In this study, Sentinel-2 data, Proba-V remote sensing data, NDVI, weather station data, ERA5, and multiple regression and FBCR models were used to examine the impacts of climate, environments, and human activities factors on vegetation dynamics for the period from 2015 to 2021. In the first phase of this study, OLS was used to evaluate the spatial association between NDVI levels and climate parameters such as air temperature, humidity, and rainfall. In the second phase of this study, FBCR was used to model and predict the spatial correlations of combinations of climate, environment, human activities, and NDVI. Our analysis of the simulation of the ERA5 model data sets and meteorological observations of temperature and total rainfall from 2000 to 2021 indicated good performance and was generally rather satisfactory. Our findings are consistent with those of a previous study by Al-Sarmi et al. [21], who found an increasing trend in air temperature between 1980 and 2013 in the northern region of the Sultanate of Oman (0.6 °C per decade^{-1}) and over the Dhofar Governorate (Salalah 0.1 °C per decade^{-1}). However, previous studies reported a decline in annual rainfall from 1980 to 2013, whereas our study found an increase in rainfall from 2018 to 2020. The trends in air temperature were high in Thumrait and Qairoon Hairiti, at a rate of 0.07 °C per year^{-1} and 0.19 °C per year^{-1}, respectively. This is due to the effect of dry, warm, inland desert air, which causes high-temperature trends to persist. In addition, air temperature trends along the coastal stations were low (at the Mirabat, Salalah Port and Sadah stations), in the range of 0.05 °C per year^{-1}, which was due to cold upwelling water that lowered air temperatures and caused temperature trends to remain low [60].

Furthermore, rainfall records revealed a clear tendency to increase from 2018 to 2020 due to the impact of frequent cyclones [61]. Several studies have reported that increased warming leads to a significant increase in tropical cyclone events and rainfall [62–64]. A study by Putnam and Broecker [65] also indicated that global warming could cause a redistribution of the Earth's rain belts in three possible ways. The first possibility is that the amount of rainfall in the tropics will increase and that in the subtropics and mid-latitudes will decrease. Another possibility is that the rain belts along the thermal equator will shift northward. A third possibility is that both scenarios will occur simultaneously. This type of repetition over a long time will likely result in a close correlation between rainfall and NDVI levels. According to our findings, NDVI was more sensitive along hilly slopes, with values > 0.4. Moreover, NDVI values were sensitive to heavy rainfall rather than moderate or light rainfall over Jabal Samhan Mountain and the eastern part of Jabal Qara Mountain. NDVI values demonstrated a significant increase and peaked in 2019 and 2020, after Cyclone Mekunu in 2018 and the deep depression (ARB 01) of May 2020. The observed dynamic change in the NDVI indicated a large contract response under climatic factors (temperature, humidity, and rainfall) in different areas of the Dhofar Governorate. In comparison to the Sadah and Mirbat stations (see Figure 6c–e), Salalah city areas had low NDVI values in the period from 2018 to 2020.

Previous research has found that climate change is one of the primary drivers of vegetation change, with human disturbance causing abrupt changes in vegetation in the study area [66]. There is also a clear trend towards grassland degeneration as a result of urbanisation in the Salalah area. Furthermore, a more recent study discovered a high correlation between the vegetation index and the building index, thereby implying that urbanisation has an indirect impact on vegetation in Dhofar's mountains, plains, and coastal areas. The study also found that urbanisation was responsible for a decline of 18.5% in other plant species found in mountainous areas during the study period [6]; however, this could also be attributed to climate change. Although many studies have found that construction development [7], population growth [67], and increased livestock [68] impact NDVI, our study revealed that climate change is one of the primary drivers of vegetation changes in the study area. Variations in air temperature and rainfall from 2015 to 2021 had varied and noticeable impacts in the regions of the Dhofar Governorate. The values of vegetation cover decreased in the western regions of Jabal Qara and along the Jabal Qamar mountain ranges (Figure 7d,e), particularly in 2019 and 2020, when the average air temperature reached its greatest values (Figure 3a).

Compared with global studies [19,69–71], this study uncovered that the spatial distribution of NDVI varies with space and time. The multiple linear regression model revealed that NDVI is significantly and positively associated with average rainfall, temperature, and humidity. In general, there is a strong linear correlation between NDVI and weather factors, with varying coefficients of determination R^2. Moreover, the rate of NDVI changes differed among the regions. The area's bedrock soil type, altitude, slope, rainfall, curvature, humidity, air temperature, topographic wetness index, distance to urban areas, aspect, distance to roads and geology, all played important roles in the distribution process of vegetation in the study area (Table 6). In addition, the observed dynamic changes in NDVI revealed a large contract response under climate factors in various areas of the Dhofar Governorate (Figure 12). Ghazanfar et al., 2003 [72] reported that the Dhofar Mountains feature numerous unique vegetation zones that are determined by climatic and topographical characteristics, such as distance from the sea, height, aspect, soil characteristics, and the quantity of precipitation from mists or rainfall and monsoon.

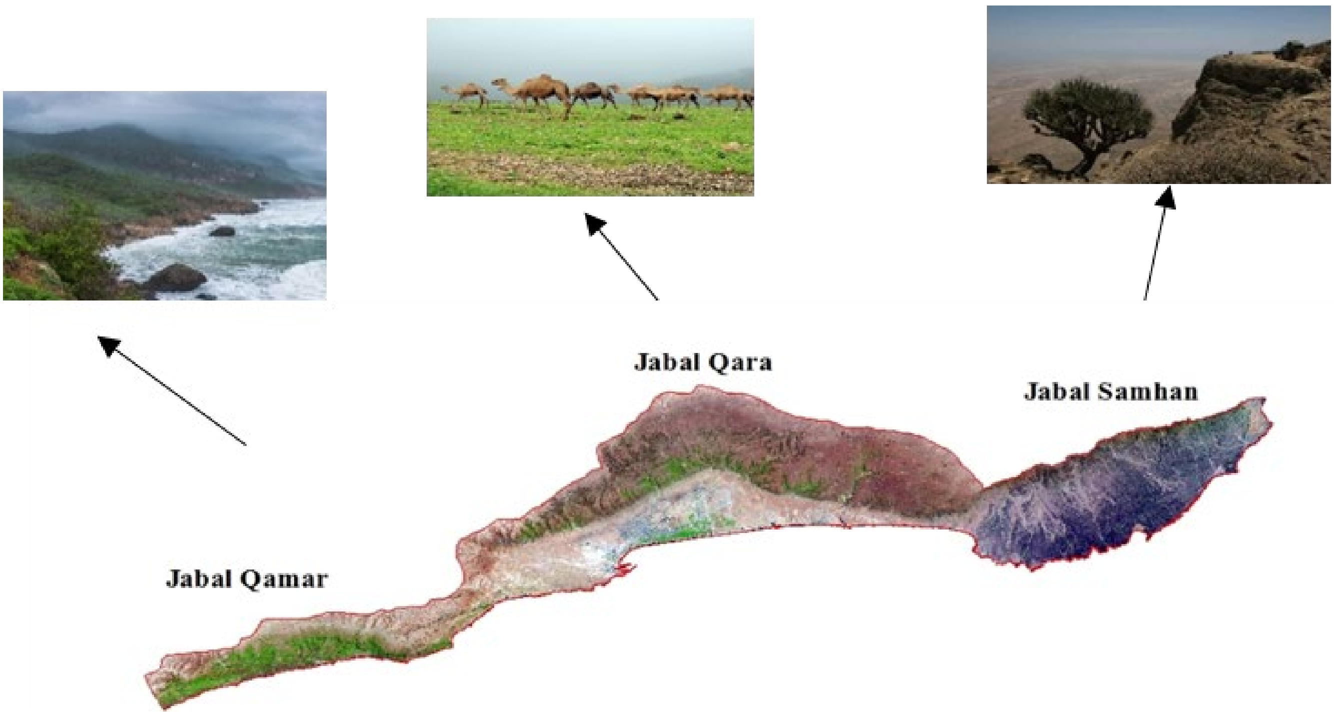

Figure 12. Climatic factors have a varied influence on the response of vegetation dynamics in the areas of the Dhofar Governorate.

The distribution of rainfall is critical in determining the richness of diverse plant species that are prevalent in the Dhofar Governorate [26]. The distribution of plants on the high dry plateau is becoming less diverse due to the blowing of hot, dry air from the desert, which hinders the formation of clouds and rain shadow (Figure 13). The current findings have significant implications for current and future availability of freshwater, with a specific emphasis on inland freshwater ecosystems. The trend of increasing vegetation may benefit the bio environment, socio-economics, and environmental sustainability [73].

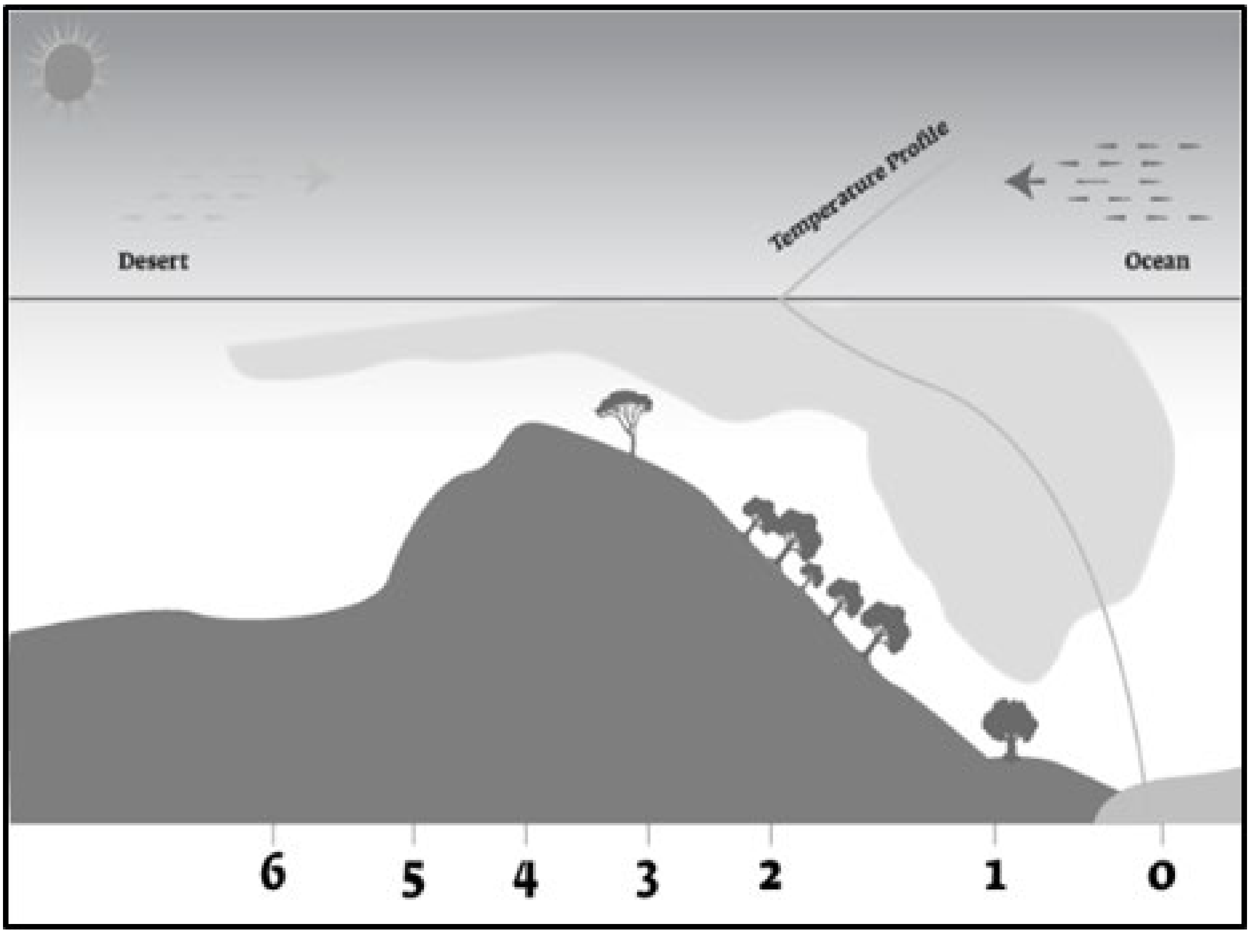

Figure 13. Climate conditions in Dhofar during the monsoon, and a diagrammatic representation of a section revealing the main habitats from sea to desert: 0—ocean; 1—coastal; 2—foothills; 3—escarpment; 4—dry plateau; 5—northern cliffs; 6—desert (modified source from source: Hildebrandt et al., 2007).

5. Conclusions

This study examined the impacts of climate, ecology, and human activities on vegetation dynamics in Dhofar Governorate, southern Oman, from 2016 to 2021 using satellite data, the ERA5, OLS, and FBCR models. The findings obtained from observation records revealed that the mean annual air temperature trends increased over all stations in air temperatures of 1 °C from 2018 to 2019. Furthermore, the study also examined the interactions between climate variables and the NDVI for the month of October for the period from 2015 to 2021. The results indicated that the trend of warming and humidification, as well as the frequency and intensity of tropical cyclones, was strengthened, thereby creating favourable conditions for the ecological restoration in the region. Moreover, there was an increase in NDVI data changes over the eastern part of Jabal Qara and along the Jabal Samhan mountain ranges, and there was synchronism between rainfall and NDVI over the study area. The current findings have significant implications for current and future freshwater availability, with a specific emphasis on inland freshwater ecosystems. Increased rainfall has a positive impact on the Dhofar Governorate's agricultural and livestock sectors, which require the use of available water, particularly economically, especially over Jabal Samhan Mountain. Furthermore, the importance of the 12 variables that influenced NDVI levels also varied. The importance of soil type, elevation, slope, rainfall, curvature, humidity, and temperature was highest, while TWI, distance to metropolitan area, aspect, distance to roadways, and geology were lowest. The increasing trend in vegetation may benefit the bio-environment, socioeconomics, and environmental sustainability in the region.

Author Contributions: This paper was the result of a broad, collaborative effort by all authors. Conceptualisation, R.A.N.; Methodology, R.A.N. and K.M.A.-K.; Formal analysis R.A.N. and K.M.A.-K.; Investigation, R.A.N., K.M.A.-K. and S.A.A.; Writing—original draft, R.A.N., K.M.A.-K. and S.A.A.; Data Curation, R.A.N., K.M.A.-K. and S.A.A.; Writing—review and editing, R.A.N. and K.M.A.-K.; Visualisation, R.A.N. and S.A.A.; Supervision, S.A.A.; Project administration, R.A.N. and K.M.A.-K. All authors have read and agreed to the published version of the manuscript.

Funding: This research is funded by the internal funds (IF), University of Nizwa, Sultanate of Oman (A/2021-2022-UoN/1/UCASA/IF) and external funds, Environmental Authority, Sultanate of Oman.

Institutional Review Board Statement: Not applicable.

Data Availability Statement: Not applicable.

Acknowledgments: The authors gratefully thank to the Environment Authority team (Yousuf Al-Rumhi, Zeyana Al-Omairi Moza Al-Riyam, and Fatma Khalfan Al-Azizi), Civil Aviation Authority, Ministry of Education (Mohammed Akak), National Survey Authority (Yunis Saleh Harith Bani-Oraba), and Directorate General of Dhofar Governorate for providing the facilities for supporting the related research.

Conflicts of Interest: The authors declare no conflict of interest.

References

1. Balling, R.C., Jr.; Klopatek, J.M.; Hildebrandt, M.L.; Moritz, C.K.; Watts, C.J. Impacts of Land Degradation on Historical Temperature Records from the Sonoran Desert. *Clim. Change* **1998**, *40*, 669–681. [CrossRef]
2. El-Beltagy, A.; Madkour, M. Impact of Climate Change on Arid Lands Agriculture. *Agric. Food Secur.* **2012**, *1*, 3. [CrossRef]
3. Doelman, J.C.; Stehfest, E. The Risks of Overstating the Climate Benefits of Ecosystem Restoration. *Nature* **2022**, *609*, E1–E3. [CrossRef]
4. Verbeeck, H.; Kearsley, E. The Importance of Including Lianas in Global Vegetation Models. *Proc. Natl. Acad. Sci. USA* **2016**, *113*, E4. [CrossRef]
5. Seto, K.C.; Güneralp, B.; Hutyra, L.R. Global Forecasts of Urban Expansion to 2030 and Direct Impacts on Biodiversity and Carbon Pools. *Proc. Natl. Acad. Sci. USA* **2012**, *109*, 16083–16088. [CrossRef]
6. Al-Mulla, Y.; Al-Ruheili, A.; Al-Lawati, A.; Parimi, K.; Ali, A.; Al-Sadi, N.; Al-Harrasi, F. Assessment of Urban Expansion's Impact on Changes in Vegetation Patterns in Dhofar, Oman, Using Remote Sensing and GIS Techniques. *IEEE Access* **2022**, *10*, 86782–86792. [CrossRef]
7. Galletti, C.S.; Turner, B.L.; Myint, S.W. Land Changes and Their Drivers in the Cloud Forest and Coastal Zone of Dhofar, Oman, between 1988 and 2013. *Reg. Environ. Change* **2016**, *16*, 2141–2153. [CrossRef]
8. Patzelt, A.; Pyšek, P.; Pergl, J.; van Kleunen, M. Alien Flora of Oman: Invasion Status, Taxonomic Composition, Habitats, Origin, and Pathways of Introduction. *Biol. Invasions* **2022**, *24*, 955–970. [CrossRef]
9. Weiskopf, S.R.; Rubenstein, M.A.; Crozier, L.G.; Gaichas, S.; Griffis, R.; Halofsky, J.E.; Hyde, K.J.W.; Morelli, T.L.; Morisette, J.T.; Muñoz, R.C.; et al. Climate Change Effects on Biodiversity, Ecosystems, Ecosystem Services, and Natural Resource Management in the United States. *Sci. Total Environ.* **2020**, *733*, 137782. [CrossRef]
10. Wu, Z.Y.; Lu, G.H.; Wen, L.; Lin, C.A. Reconstructing and Analyzing China's Fifty-Nine Year (1951-2009) Drought History Using Hydrological Model Simulation. *Hydrol. Earth Syst. Sci.* **2011**, *15*, 2881–2894. [CrossRef]
11. Diffenbaugh, N.S.; Davenport, F.V.; Burke, M. Historical Warming Has Increased U.S. Crop Insurance Losses. *Environ. Res. Lett.* **2021**, *16*, 084025. [CrossRef]
12. Hoffmann, W.A.; Schroeder, W.; Jackson, R.B. Positive Feedbacks of Fire, Climate, and Vegetation and the Conversion of Tropical Savanna. *Geophys. Res. Lett.* **2002**, *29*, 91–94. [CrossRef]
13. Vicente-Serrano, S.M.; Gouveia, C.; Camarero, J.J.; Beguería, S.; Trigo, R.; López-Moreno, J.I.; Azorín-Molina, C.; Pasho, E.; Lorenzo-Lacruz, J.; Revuelto, J.; et al. Response of Vegetation to Drought Time-Scales across Global Land Biomes. *Proc. Natl. Acad. Sci. USA* **2013**, *110*, 52–57. [CrossRef] [PubMed]

14. Ning, T.; Liu, W.; Lin, W.; Song, X. NDVI Variation and Its Responses to Climate Change on the Northern Loess Plateau of China from 1998 to 2012. *Adv. Meteorol.* **2015**, *2015*, 725427. [CrossRef]
15. Wu, D.; Zhao, X.; Liang, S.; Zhou, T.; Huang, K.; Tang, B.; Zhao, W. Time-Lag Effects of Global Vegetation Responses to Climate Change. *Glob. Chang. Biol.* **2015**, *21*, 3520–3531. [CrossRef]
16. Guo, J.; Hu, Y.; Xiong, Z.; Yan, X.; Ren, B.; Bu, R. Spatiotemporal Variations of Growing-Season NDVI Associated with Climate Change in Northeastern China's Permafrost Zone. *Polish J. Environ. Stud.* **2017**, *26*, 1521–1529. [CrossRef]
17. Liu, Y.; Li, Y.; Li, S.; Motesharrei, S.; Lee, C.-T.; Huete, A.R.; Roy, S.; Thenkabail, P.S. Spatial and Temporal Patterns of Global NDVI Trends: Correlations with Climate and Human Factors. *Remote Sens.* **2015**, *7*, 13233–13250. [CrossRef]
18. Schultz, P.A.; Halpert, M.S. Global Analysis of the Relationships among a Vegetation Index, Precipitation and Land Surface Temperature. *Int. J. Remote. Sens.* **1995**, *16*, 2755–2777. [CrossRef]
19. Abdul-Wahab, S.A. Analysis of Thermal Inversions in the Khareef Salalah Region in the Sultanate of Oman. *J. Geophys. Res. Atmos.* **2003**, *108*, 4274. [CrossRef]
20. Ahmed, M.; Choudri, B.S. Climate Change in Oman: Current Knowledge and Way Forward. *Educ. Bus. Soc. Contemp. Middle East. Issues* **2012**, *5*, 228–236. [CrossRef]
21. Al-Sarmi, S.; Al-Yahyai, S.; Al-Maskari, J.; Charabi, Y.; Choudri, B.S. Recent Observed Climate Change Over Oman. In *Springer Water*; Springer International Publishing: Berlin/Heidelberg, Germany, 2017; pp. 89–100. [CrossRef]
22. Al-Kalbani, M.S.; Price, M.F.; Abahussain, A.; Ahmed, M.; O'Higgins, T. Vulnerability Assessment of Environmental and Climate Change Impacts on Water Resources in Al Jabal Al Akhdar, Sultanate of Oman. *Water* **2014**, *6*, 3118–3135. [CrossRef]
23. Wang, D.; Zhao, H. Estimation of Phytoplankton Responses to Hurricane Gonu over the Arabian Sea Based on Ocean Color Data. *Sensors* **2008**, *8*, 4878. [CrossRef] [PubMed]
24. Knaff, J.A.; Demaria, M.; Molenar, D.A.; Sampson, C.R.; Seybold, M.G. An Automated, Objective, Multiple-Satellite-Platform Tropical Cyclone Surface Wind Analysis. *J. Appl. Meteorol. Climatol.* **2011**, *50*, 2149–2166. [CrossRef]
25. Sarker, M.A. Numerical Modelling of Waves and Surge from Cyclone Mekunu (May 2018) in the Arabian Sea. *J. Atmos. Sci. Res.* **2020**, *2*, 12–20. [CrossRef]
26. El-Sheikh, M.A. Weed Vegetation Ecology of Arable Land in Salalah, Southern Oman. *Saudi J. Biol. Sci.* **2013**, *20*, 291–304. [CrossRef]
27. Al-Habsi, M.; Gunawardhana, L.; Al-Rawas, G. Trend Analysis of Climate Variability in Salalah, Oman. *Int. J. Stud. Res. Technol. Manag.* **2014**, *2*, 168–171.
28. Prathapar, S.A.; Khan, M.; Mbaga, M.D. The Potential of Transforming Salalah into Oman's Vegetables Basket. In *Environmental Cost and Face of Agriculture in the Gulf Cooperation Council Countries*; Springer: Berlin/Heidelberg, Germany, 2014; pp. 83–94.
29. Halofsky, J.E.; Hemstrom, M.A.; Conklin, D.R.; Halofsky, J.S.; Kerns, B.K.; Bachelet, D. Assessing Potential Climate Change Effects on Vegetation Using a Linked Model Approach. *Ecol. Modell.* **2013**, *266*, 131–143. [CrossRef]
30. Edmond Moeletsi, M.; Phumlani Shabalala, Z.; De Nysschen, G.; Walker, S. Evaluation of an Inverse Distance Weighting Method for Patching Daily and Dekadal Rainfall over the Free State Province, South Africa. *Water SA* **2016**, *42*, 466–474. [CrossRef]
31. Stocker, T.F.; Qin, D.; Plattner, G.-K.; Tignor, M.M.B.; Allen, S.K.; Boschung, J.; Nauels, A.; Xia, Y.; Bex, V.; Midgley, P.M. *Climate Change 2013: The Physical Science Basis. Contribution of Working Group I to the Fifth Assessment Report of IPCC the Intergovernmental Panel on Climate Change*; Cambridge University Press: Cambridge, UK, 2014.
32. Martin, C.A. *Regional Frequency Analysis of Seasonal Rainfall and Snowfall for the Southern Interior of British Columbia*; Thompson Rivers University: Kamloops, BC, Canada, 2015.
33. Hersbach, H.; Bell, B.; Berrisford, P.; Hirahara, S.; Horányi, A.; Muñoz-Sabater, J.; Nicolas, J.; Peubey, C.; Radu, R.; Schepers, D.; et al. The ERA5 Global Reanalysis. *Q. J. R. Meteorol. Soc.* **2020**, *146*, 1999–2049. [CrossRef]
34. Jiao, D.; Xu, N.; Yang, F.; Xu, K. Evaluation of Spatial-Temporal Variation Performance of ERA5 Precipitation Data in China. *Sci. Rep.* **2021**, *11*, 17956. [CrossRef]
35. Tetzner, D.; Thomas, E.; Allen, C. A Validation of ERA5 Reanalysis Data in the Southern Antarctic Peninsula—Ellsworth Land Region, and Its Implications for Ice Core Studies. *Geosciences* **2019**, *9*, 289. [CrossRef]
36. Alves, M.; Nadeau, D.F.; Music, B.; Anctil, F.; Parajuli, A. On the Performance of the Canadian Land Surface Scheme Driven by the ERA5 Reanalysis over the Canadian Boreal Forest. *J. Hydrometeorol.* **2020**, *21*, 1383–1404. [CrossRef]
37. Hassler, B.; Lauer, A. Comparison of Reanalysis and Observational Precipitation Datasets Including ERA5 and WFDE5. *Atmosphere* **2021**, *12*, 1462. [CrossRef]
38. Frampton, W.J.; Dash, J.; Watmough, G.; Milton, E.J. Evaluating the Capabilities of Sentinel-2 for Quantitative Estimation of Biophysical Variables in Vegetation. *ISPRS J. Photogramm. Remote Sens.* **2013**, *82*, 83–92. [CrossRef]
39. Al-Kindi, K.M.; Alabri, Z.; Al-Farsi, M. Geospatial Detection of Ommatissus Lybicus de Bergevin Using Spatial and Machine Learning Techniques. *Remote Sens. Appl. Soc. Environ.* **2022**, *28*, 100814. [CrossRef]
40. Rouse, J.W.J.; Haas, R.H.; Schell, J.A.; Deering, D.W.; Rouse, J.W.J.; Haas, R.H.; Schell, J.A.; Deering, D.W. Monitoring Vegetation Systems in the Great Plains with Erts. *NASSP* **1974**, *351*, 309.

41. Myneni, R.B.; Hall, F.G.; Sellers, P.J.; Marshak, A.L. Interpretation of Spectral Vegetation Indexes. *IEEE Trans. Geosci. Remote Sens.* **1995**, *33*, 481–486. [CrossRef]
42. Purevdorj, T.S.; Tateishi, R.; Ishiyama, T.; Honda, Y. Relationships between Percent Vegetation Cover and Vegetation Indices. *Int. J. Remote Sens.* **2010**, *19*, 3519–3535. [CrossRef]
43. Dash, J.; Curran, P.J. The MERIS Terrestrial Chlorophyll Index. *Int. J. Remote Sens.* **2004**, *25*, 5403–5413. [CrossRef]
44. Quan, X.; Wang, Y.; Xiong, W.; He, M.; Yang, Z.; Lin, C. Description of Microbial Community Structure of Sediments from the Daliao River Water System and Its Estuary (NE China) by Application of Fluorescence in Situ Hybridization. *Environ. Earth Sci.* **2010**, *61*, 1725–1734. [CrossRef]
45. Liu, Y.; Liang, X.; Dong, W.; Fang, Y.; Lv, J.; Zhang, T.; Fiskesund, R.; Xie, J.; Liu, J.; Yin, X. Tumor-Repopulating Cells Induce PD-1 Expression in CD8+ T Cells by Transferring Kynurenine and AhR Activation. *Cancer Cell* **2018**, *33*, 480–494. [CrossRef]
46. Lobell, D.B.; Hicke, J.A.; Asner, G.P.; Field, C.B.; Tucker, C.J.; Los, S.O. Satellite Estimates of Productivity and Light Use Efficiency in United States Agriculture, 1982–98. *Glob. Chang. Biol.* **2002**, *8*, 722–735. [CrossRef]
47. Wang, F.; Wang, X.; Zhao, Y.; Yang, Z. Temporal Variations of NDVI and Correlations between NDVI and Hydro-Climatological Variables at Lake Baiyangdian, China. *Int. J. Biometeorol.* **2014**, *58*, 1531–1543. [CrossRef] [PubMed]
48. Durante, P.; Oyonarte, C.; Valladares, F. Influence of Land-Use Types and Climatic Variables on Seasonal Patterns of NDVI in Mediterranean Iberian Ecosystems. *Appl. Veg. Sci.* **2009**, *12*, 177–185. [CrossRef]
49. Del Grosso, S.J.; Parton, W.J.; Derner, J.D.; Chen, M.; Tucker, C.J. Simple Models to Predict Grassland Ecosystem C Exchange and Actual Evapotranspiration Using NDVI and Environmental Variables. *Agric. For. Meteorol.* **2018**, *249*, 1–10. [CrossRef]
50. Pouliot, D.; Latifovic, R.; Olthof, I. Trends in Vegetation NDVI from 1 Km AVHRR Data over Canada for the Period 1985–2006. *Int. J. Remote Sens.* **2009**, *30*, 149–168. [CrossRef]
51. Al-Kindi, K.M.; Kwan, P.; Andrew, N.R.; Welch, M. Remote Sensing and Spatial Statistical Techniques for Modelling *Ommatissus lybicus* (Hemiptera: Tropiduchidae) Habitat and Population Densities. *PeerJ* **2017**, *2017*, e3752. [CrossRef]
52. Oksanen, J.; Blanchet, F.G.; Kindt, R.; Legendre, P.; Minchin, P.R.; O'hara, R.B.; Simpson, G.L.; Solymos, P.; Stevens, M.H.H.; Wagner, H. Package 'Vegan. ' *Community Ecol. Packag. Version* **2013**, *2*, 1–295.
53. Borcard, D.; Gillet, F.; Legendre, P. *Numerical Ecology with R*; Springer: Berlin/Heidelberg, Germany, 2011; Volume 2.
54. Breiman, L. Bagging Predictors. *Mach. Learn.* **1996**, *24*, 123–140. [CrossRef]
55. Breiman, L. Stacked Regressions. *Mach. Learn.* **1996**, *24*, 49–64. [CrossRef]
56. Liu, Y.; Wang, Y.; Zhang, J. New Machine Learning Algorithm: Random Forest. In Proceedings of the Third International Conference on Information Computing and Applications, Chengde, China, 14–16 September 2012; pp. 246–252.
57. Breiman, L. Random Forests. *Mach. Learn.* **2001**, *45*, 5–32. [CrossRef]
58. Breiman, L. Using Iterated Bagging to Debias Regressions. *Mach. Learn.* **2001**, *45*, 261–277. [CrossRef]
59. Pan, S.; Zhao, X.; Yue, Y. Spatiotemporal Changes of NDVI and Correlation with Meteorological Factors in Northern China from 1985–2015. *E3S Web Conf.* **2019**, *131*, 01040. [CrossRef]
60. Praveen, V.; Ajayamohan, R.S.; Valsala, V.; Sandeep, S. Intensification of Upwelling along Oman Coast in a Warming Scenario. *Geophys. Res. Lett.* **2016**, *43*, 7581–7589. [CrossRef]
61. Andreou, G.M.; Westley, K.; Huigens, H.O.; Blue, L. Exploring the Impact of Tropical Cyclones on Oman's Maritime Cultural Heritage Through the Lens of Al-Baleed, Salalah (Dhofar Governorate). *J. Marit. Archaeol.* **2022**, *17*, 465–486. [CrossRef]
62. Villarini, G.; Lavers, D.A.; Scoccimarro, E.; Zhao, M.; Wehner, M.F.; Vecchi, G.A.; Knutson, T.R.; Reed, K.A. Sensitivity of Tropical Cyclone Rainfall to Idealized Global-Scale Forcings. *J. Clim.* **2014**, *27*, 4622–4641. [CrossRef]
63. Guzman, O.; Jiang, H. Global Increase in Tropical Cyclone Rain Rate. *Nat. Commun.* **2021**, *12*, 5344. [CrossRef]
64. Utsumi, N.; Kim, H. Observed Influence of Anthropogenic Climate Change on Tropical Cyclone Heavy Rainfall. *Nat. Clim. Chang.* **2022**, *12*, 436–440. [CrossRef]
65. Putnam, A.E.; Broecker, W.S. Human-Induced Changes in the Distribution of Rainfall. *Sci. Adv.* **2017**, *3*, e1600871. [CrossRef]
66. MacLaren, C.A. Climate Change Drives Decline of Juniperus Seravschanica in Oman. *J. Arid Environ.* **2016**, *128*, 91–100. [CrossRef]
67. Shammas, M.I. The Effectiveness of Artificial Recharge in Combating Seawater Intrusion in Salalah Coastal Aquifer, Oman. *Environ. Geol.* **2008**, *55*, 191–204. [CrossRef]
68. Soares, P.M.M.; Lima, D.C.A.; Nogueira, M.; Gopinath, A.; Al Quri, K.; Hussein, M.A.; Mahmoud, H.; Ahmed, S.; Moosa, S. Over-Grazing in the Dhofar Mountain Region: A Major Sustainability Challenge. *IOP Conf. Ser. Earth Environ. Sci* **2022**, *1055*, 012021. [CrossRef]
69. Chuai, X.W.; Huang, X.J.; Wang, W.J.; Bao, G. NDVI, Temperature and Precipitation Changes and Their Relationships with Different Vegetation Types during 1998–2007 in Inner Mongolia, China. *Int. J. Climatol.* **2013**, *33*, 1696–1706. [CrossRef]
70. Schmidt, M.; Klein, D.; Conrad, C.; Dech, S.; Paeth, H. On the Relationship between Vegetation and Climate in Tropical and Northern Africa. *Theor. Appl. Climatol.* **2014**, *115*, 341–353. [CrossRef]
71. Ding, M.; Zhang, Y.; Liu, L.; Zhang, W.; Wang, Z.; Bai, W. The Relationship between NDVI and Precipitation on the Tibetan Plateau. *J. Geogr. Sci.* **2007**, *17*, 259–268. [CrossRef]

72. Mosti, S.; Raffaelli, M.; Tardelli, M. A Contribution to the Flora of Wadi Andur (Dhofar, Southern Oman). *Webbia* **2006**, *61*, 253–260. [CrossRef]
73. Polasky, S.; Kling, C.L.; Levin, S.A.; Carpenter, S.R.; Daily, G.C.; Ehrlich, P.R.; Heal, G.M.; Lubchenco, J. Role of Economics in Analyzing the Environment and Sustainable Development. *Proc. Natl. Acad. Sci. USA* **2019**, *116*, 5233–5238. [CrossRef]